Mechanical Properties and Microstructural Features of Direct Laser-Deposited Ti-6Al-4V

LINKAN BIAN,[1] SCOTT M. THOMPSON,[2,3] and NIMA SHAMSAEI[2,3,4]

1.—Department of Industrial & Systems Engineering, Mississippi State University, Mississippi State, MS 39762, USA. 2.—Department of Mechanical Engineering, Mississippi State University, PO Box 9552, Mississippi State, MS 39762, USA. 3.—Center for Advanced Vehicular Systems (CAVS), Mississippi State University, Mississippi State, MS 39762, USA. 4.—e-mail: shamsaei@me.msstate.edu

Direct laser deposition (DLD) is a means to additively manufacture metallic, functional parts via blown powder (or wire) and in situ laser delivery. Despite the various research efforts in characterization of post-manufactured DLD parts and in optimizing the DLD process, there are still areas that need to be further explored to promote the widespread adaption and utilization of DLD parts for engineering application. This article aims to review the mechanical properties of Ti-6Al-4V parts manufactured via DLD, including tensile and fatigue characteristics and microstructural features. These mechanical properties will be related with DLD process parameters (e.g., laser power, traverse speed, etc.) and resultant phenomena such as melt pool dynamics and part thermal history. Because fatigue is a main failure mode of parts in many engineering applications, the fatigue behavior of Ti-6Al-4V parts fabricated via DLD is highlighted and discussed in detail.

INTRODUCTION

Additive manufacturing (AM) is the process of joining materials to make objects from three-dimensional (3D) model data in a layer-wise manner. It is distinctly different from many traditional manufacturing processes in that it allows for on-demand generation of customized parts. For individualized parts and small-quantity productions, the AM process allows for the opportunity to significantly reduce manufacturing times and costs. Furthermore, AM shows promise to more easily generate novel components and structures with complex geometries and heterogeneous compositions. In terms of mass production, AM has the potential to compress the supply chain and to reduce the amount of material waste—especially as compared to traditional "subtractive" manufacturing.

A major category of AM is direct laser deposition (DLD), which is typically accomplished via a blown powder system such as Laser Engineered Net Shaping (LENS). For LENS, a high-power laser (e.g., Nd:YAG) creates a molten puddle (melt pool) on the substrate surface in which powder is then injected. Because DLD does not rely on the presence of a pre-deposited layer of metallic powder (e.g., laser powder bed fusion), it may be used as a means to repair parts via cladding. In addition, because of the combined material/energy delivery method, DLD can be readily used for multi-material/preform deposition allowing for the generation of functionally graded/composed parts with varying alloy concentrations. In addition, material preform mixing can be accomplished with DLD, such as coaxial powder delivery and lateral wire feeding.[1,2]

DLD can be used for the additive manufacture of a variety of metals and even ceramics, including Inconel 625, stainless steels, H13 tool steel, titanium alloys, tungsten, and more.[3–8] Much attention has been given to the DLD fabrication of Ti-6Al-4V due to the unique advantages of this alloy. Some advantages include high strength and stiffness-to-weight ratio, high melting point, high toughness, low value of coefficient of thermal expansion (CTE), excellent corrosion, creep and wear resistance, and biocompatibility.[9] However, because of the many involved process variables in laser-based, AM techniques (such as laser power, scanning speed, scanning strategy, layer thickness, hatching pitch, etc.), predicting the microstructural/mechanical properties of DLD fabricated parts are still a major challenge.

To achieve enhanced mechanical properties at critical locations within/along DLD fabricated parts, it is essential to understand and characterize how DLD process parameters (e.g., laser power, traverse speed, powder feed rate, hatching pitch, layer thickness, etc.) affect the part's thermal history, solidification, and eventual microstructural/mechanical properties. The relationship among these phenomena/parameters is presented schematically in Fig. 1. As shown in Fig. 1, the process parameters affect the cooling rate, thermal gradient, and generally, the thermal history of DLD fabricated parts. This complex thermal history drives solidification and, consequently, impacts the resultant microstructure, porosity, and residual stresses inherent in the DLD fabricated part. Mechanical properties, especially fatigue and durability performance, are extremely sensitive to these process-initiated characteristics (e.g., microstructure, porosity, etc.) and thus motivates the study of the DLD process and post-DLD part behavior.

The typical DLD process is shown in Fig. 2. A molten pool (or melt pool) of metal is formed by combining a focused, power-controlled laser and a blown powder material stream (at a controlled powder feed rate). The laser is delivered coaxially, normal to the melt pool, while the blown powder is introduced either by a singular nozzle or multiple nozzles. For example, a LENS machine[10] uses four nozzles to accomplish DLD, and this increases the powder deposition efficiency significantly. The end result of the laser/powder/part interaction is a superheated melt pool[11–13] that moves along with the laser—at a relative, traverse speed between substrate and laser—and solidifies to form the various layers for the additive-based manufacture. This interaction, i.e., through variation of laser power,

traverse speed, and powder feed rate, can be tailored as to produce, for example, specific layer thicknesses, patterns, and melt pool size/shapes that ultimately affect microstructure, hardness, tensile, and fatigue properties. Inert gas is used to minimize oxidization atop the powder/melt pool/part while processing at the elevated temperatures to ensure better layer-to-layer adhesion and part quality. A thermal monitoring system, which may be composed of infrared cameras and/or pyrometers, can be integrated into/outside the DLD machine.[3,14–17] Such thermal monitoring can be used for "closing-the-loop" on the DLD process—providing a means for real-time, feedback control of melt pool/part temperature and morphology.[18,19]

The aim of this article is to review the mechanical properties, microstructural features, and causal thermal behavior of Ti-6Al-4V parts fabricated via DLD. Microstructural and mechanical properties, as well as thermal history during manufacturing, are discussed in the following sections.

MECHANICAL PROPERTIES

Mechanical tests, such as tensile, hardness/microhardness, and fatigue, are commonly used to evaluate the performance of various parts prior to their widespread application. Tensile tests can be conducted to examine the strength and elongation-to-failure of a material under static loading, whereas fatigue tests can be conducted to investigate the behavior of material under cyclic loading. In engineering design, failure is usually associated with fracture or excessive deformation. Hence, tensile and fatigue tests of a material are crucial in determining vital properties required for any design.

The tensile properties of DLD fabricated Ti-6Al-4V (Ti-6Al-4V/DLD) parts are typically similar, or even superior, to those of wrought and cast materials by virtue of the high cooling rates experienced during DLD. Instantaneous cooling rates can be on the order of 5000–10000 K/s,[15,20] whereas cooling rates near 1500 K/s have also been measured and reported.[21] These relatively high cooling rates foster the development of extremely fine microstructures that distribute uniformly throughout the parts' volume.[20,22] Although the ultimate tensile and yield strengths of Ti-6Al-4V/DLD parts are higher than those of wrought materials in most cases, the elongation to failure and ductility is typically lower. This implies higher strength and lower ductility in DLD-produced titanium alloys than in their wrought counterparts, as presented in Fig. 3a.

Post-manufacturing heat treatments, such as hot isostatic pressing (HIP), can be used to reduce part porosity and increase the density of materials via elevated temperature and isostatic gas pressure. Adequate densification via the HIP process can lead to a higher ductility and elongation to rupture.[23] Furthermore, lower levels of anisotropy are ob-
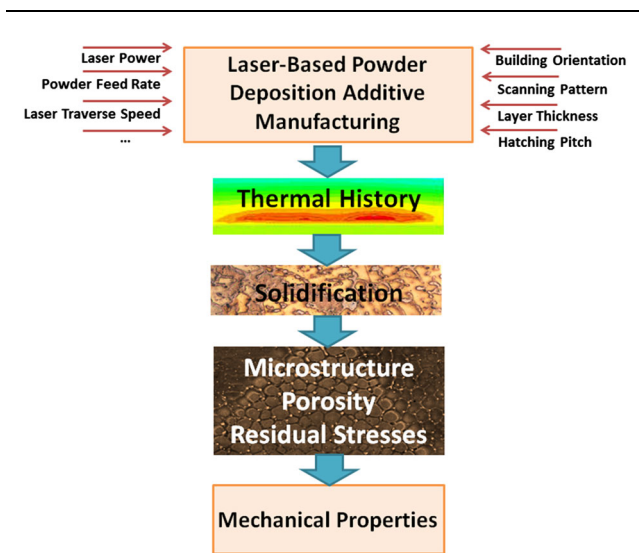

Fig. 1. Schematic of relationships among process parameters, thermal history, microstructure, and fatigue behavior in direct laser deposition.
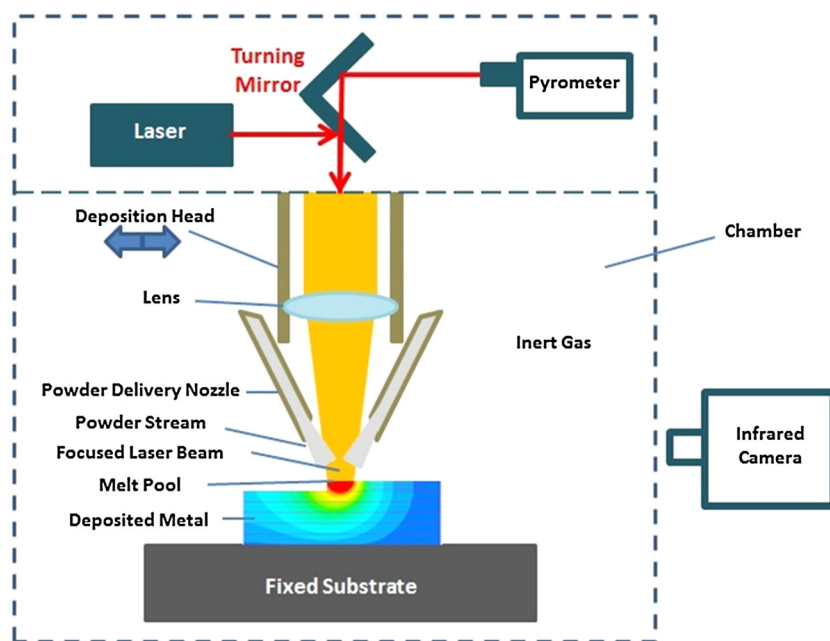
Fig. 2. The direct laser deposition process.

served from parts treated via HIP, as opposed to as-built or regular heat-treated parts, as presented in Fig. 3a. This indicates that porosity may play a crucial role in the anisotropic behavior of laser deposited parts, especially when measuring/quantifying ultimate strength. The effects of mechanical or crystallographic texture on anisotropy are still noticeable when measuring the yield strength after the HIP process. Anisotropy in the mechanical texture may result from existent columnar grain morphology, by having smaller effective grain sizes in direction perpendicular to the columnar grains than in the parallel direction. In general, anisotropy in the crystallographic texture is a result of the relatively high anisotropy of the hexagonal crystal structure in titanium alloys.[23]

The effects of surface condition and heat treatment on Ti-6Al-4V/DLD samples are presented in Fig. 3b where it may be seen that improving the surface quality by post-DLD machining can increase the tensile strength of laser-fabricated components. These observed tensile strength enhancements may be attributed to the improved surface quality and/or removing the surface and subsurface material with dislike microstructure from the core material, a result of different radial cooling rates. Moreover, tensile residual stresses, which mainly exist at the surface of parts, can be removed by the post-manufacturing machining. A careful examination of core and surface microstructures can be performed to better understand the effect of surface machining on tensile properties. Furthermore, machining and heat treatment can effectively reduce the effect of building orientation by homogenizing the directional porosity and microstructure. Heat

treatment significantly improves the ductility of DLD components, up to the wrought materials, by coarsening the microstructure and providing stress relief, as shown in Fig. 3b.

Fatigue, a critical characteristic in the analysis and design of engineering materials, is a main failure mode in many mechanical applications with repeated/cyclic loading. The load-to-failure via fatigue is typically much lower than what is required to cause failure of materials under monotonic (non-cyclic) loads. Cyclic damage leads to local cracking and causes fracture after a sufficient number of fluctuations. Generally, fatigue life less than 10^3 cycles is considered as low cycle fatigue (LCF, or short-life regime), the fatigue life of $10^3 < N_f < 10^5$ cycles is classified as mid-cycle fatigue (or mid-life regime), and $N_f > 10^5$ is categorized as high-cycle fatigue (HCF, or long-life regime).

The fatigue behavior of Ti-6Al-4V/DLD parts is complex and still not well understood. Ostentatiously inconsistent results have been reported in the literature. As shown in Fig. 4, high cycle fatigue data have been reported;[23,24] Grylls[24] reported comparable (or superior) fatigue behavior for Ti-6Al-4V/DLD to wrought materials, and Kobryn and Semiatin[23] reported significantly lower fatigue strength for Ti-6Al-4V/DLD. These inconsistencies may be attributed to many factors that affect fatigue behavior; however, different microstructures and porosity levels may be the main influential factors.

Fatigue behavior is typically related to microstructural features (i.e., grain size and morphology, as well as presence of impurities such as voids and inclusions). Finer microstructures generally exhibit better crack-initiation resistance com-
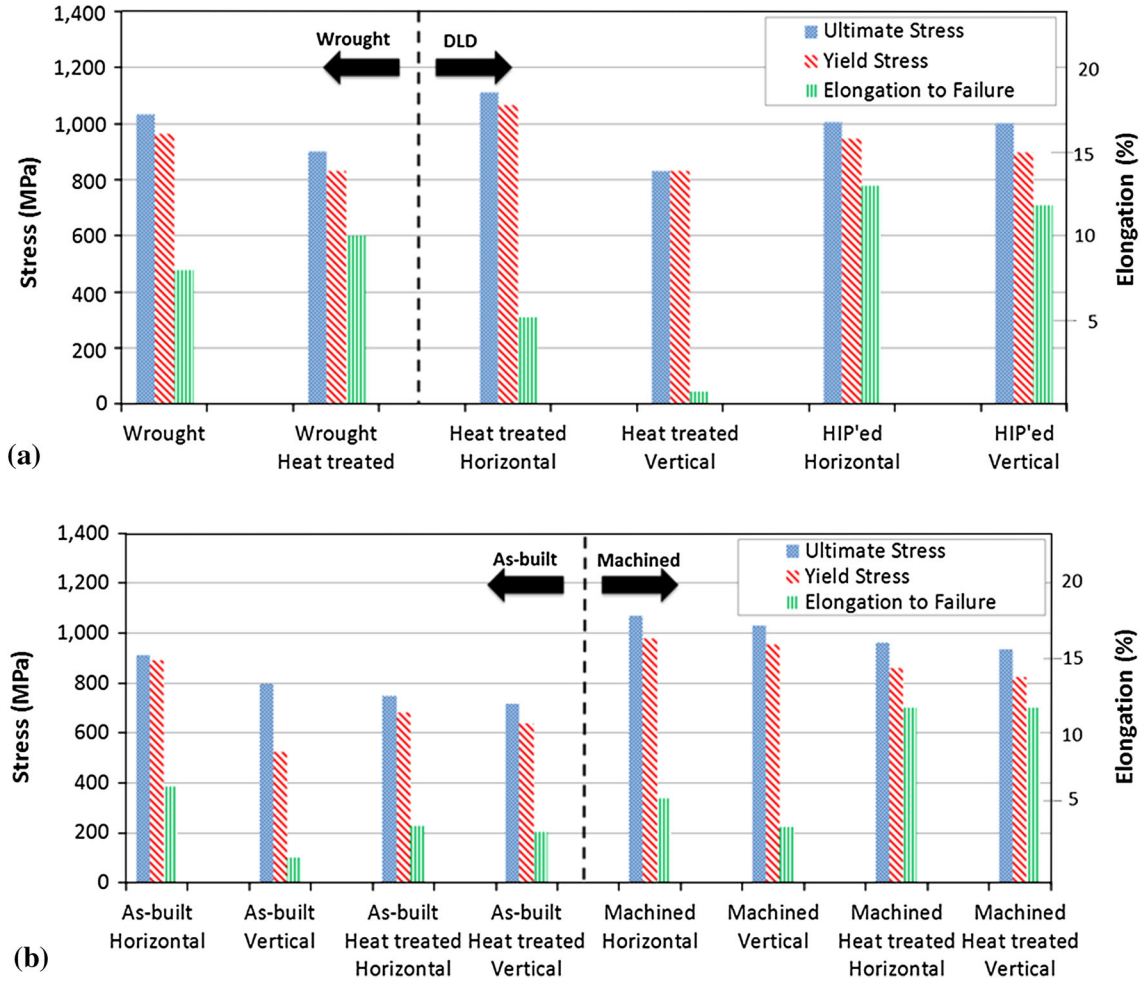
Fig. 3. (a) Tensile properties of Ti-6Al-4V/DLD[23] in different building orientations after heat treatment and HIP process compared to wrought materials[63] and (b) effect of machining and heat treatment on tensile properties of Ti-6Al-4V/DLD in different orientations[32].
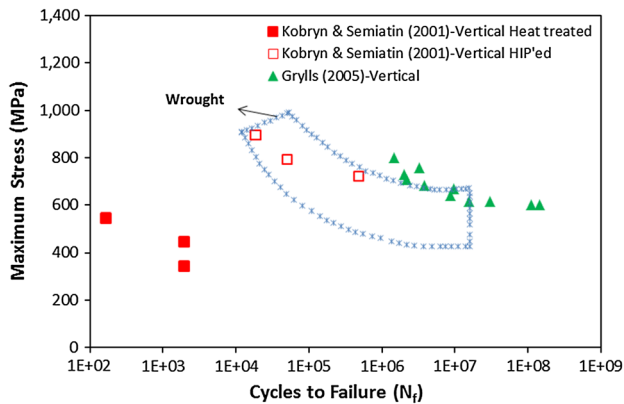

Fig. 4. Comparison of S–N data of different studies for the LENS-produced Ti-6Al-4V samples printed in vertical direction[23,24] to the wrought materials[63].

ture usually exhibit less resistance to crack propagation resulting in inferior LCF behavior; as compared with coarser microstructures with a rougher crack path.[25,26] The thermal history during the DLD process has a significant effect on the grain structure and volume fraction of α and β constituents. The blocking effects on the dislocations' movement of the grain boundaries may improve the resistance to deformation, resulting in an increased stress response and cyclic hardening in the material. However, the softer α grain boundary may accelerate the crack growth rate in Ti-6AL-4V. The detrimental effects of the α grain soft zone on crack growth resistance may be reduced by an appropriate heat treatment process.[27]

Porosity is another measurement that determines the fatigue behavior of DLD parts. Pores may greatly affect the fatigue behavior by creating stress concentrations at their walls. Local microscopic stresses larger than the yield strength cause local plastic deformation and can lead to fatigue crack initiation under cyclic loading. In contrast to LCF, crack initiation is more contributive to the total fa-

pared with coarser microstructures. However, materials with finer microstructure promote a flatter crack path that results in higher crack-growth rates. Therefore, materials with finer microstruc-

tigue lifetime in HCF. Therefore, any variations in microstructure discontinuity (caused by defects), such as cracks, porosity, and unmelted powder, can accelerate the nucleation of the crack and may consequently decrease the total fatigue life in the HCF regime.[27,28] It has been found that the micropore size and its distance from the surface strongly affect the HCF life of titanium alloys.[29] Fatigue life decreases with an increase in pore size and a decrease in its distance with respect to the surface. In addition, a pore's location is a more influential parameter than the pore size on the fatigue resistance at lower stress levels (i.e., HCF).[27]

Post-manufacturing processing, such as heat treatment, influences the microstructure and, therefore, fatigue behavior of Ti-6Al-4V/DLD parts. At room temperature, the microstructure of Ti-6Al-4V, which consists of both hexagonal-close-packed (hcp) α and body-centered-cubic (bcc) β phases, varies based on the thermal history of the alloy. Heat treatments affect the distribution, size, and shape of the α phase; however, no significant effect on the prior-β grains may be expected.[30] Thermal treatment of laser-deposited Ti-6Al-4V parts close to the solutionizing temperature (900°C to 970°C for this alloy) changes the acicular α-β microstructure to columnar β grains, as well as coarsening the Widmanstätten α grains and providing for lower porosities.[31,32] Different heat treatments may result in completely different fatigue behaviors. For example, Kobryn and Semiatin's parts[23] were stress relieved in vacuum for 2 h at 700°C to 730°C, whereas Grylls[24] did not report any heat treatments.

Anisotropic (i.e., directionally dependent) behavior has also been reported in fatigue resistance of laser-deposited Ti-6Al-4V parts.[23] In general, vertically built parts show significantly lower fatigue strength than horizontally built parts, as presented in Fig. 4. Various time–temperature paths imposed by the laser may cause directional and inhomogeneous cooling behavior of the melt pool, resulting in different microstructural features, residual stresses, and consequently, fatigue behavior. The parts fabricated in a vertical direction can contain extensive porosity compared with those built in horizontal directions.[23] The parts processed via HIP exhibit much smaller anisotropic effects than the heat-treated ones, as presented in Fig. 5. Such observations indicate that the amount of porosity plays an important role in the anisotropic behavior of laser-deposited parts. It is clear that the effects of different manufacturing and post-manufacturing parameters on the anisotropic behavior of laser-deposited parts are not currently well understood; thus, further investigations are required.

Manufacturing process parameters, such as laser power, traverse speed, powder feed rate, and layer thickness, greatly influence the thermal history, microstructure, bonding between layers, pore size, and shape, and consequently, the fatigue resistance
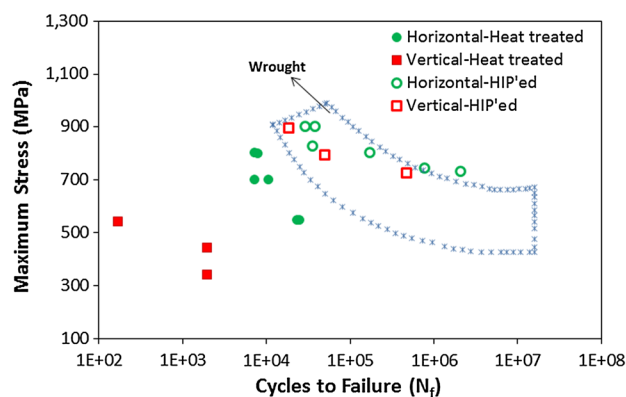

Fig. 5. Comparison of fatigue strengths for LENS-produced Ti-6Al-4V in different building orientations for both heat-treated and hot isostatically pressed parts[23].

of DLD fabricated products. Residual stresses that accumulate in parts produced by laser deposition are another thermal-path dependent phenomenon that may greatly affect the fatigue behavior of the product.[22] In addition to variability in microstructure and porosity, differences in the reported fatigue strength for Ti-6Al-4V/DLD[23,24] may also be attributed to variability in manufacturing process parameters and in fatigue test setups. Various specimens' size, shape, and surface quality, might also be responsible for inconsistencies of fatigue data presented in Fig. 4. Therefore, because of the many complicated, interdependent parameters in the DLD process and variability in preparing specimens, test setups, and post-manufacturing process, it is difficult to compare these reported fatigue studies. Selecting the process parameters and conditions to achieve the desired fatigue behavior requires further investigation.

MICROSTRUCTURAL FEATURES

Microstructural features (e.g., grain size and morphology) of laser-deposited Ti-6Al-4V parts are sensitive to thermal history. This includes local thermal gradients, cooling rates, and reheating cycles experienced during processing, as well as post-manufacturing heat treatments. Several studies in the literature have investigated the effects of manufacturing/post-manufacturing process parameters on the resultant microstructure of Ti-6Al-4V.[23,33,34] However, it is still unclear how to apply these findings to fabricate titanium parts with different geometries as the microstructure primarily depends on the thermal history, which varies with distinct part geometries.

The solidified microstructure depends on the local solidification rate of the melt pool, the temperature gradient at the solid–liquid interface, and the cooling rate.[35,36] Different values of these parameters can result in three major structure morphologies in Ti-6Al-4V/DLD parts: columnar (elongated grain morphology), columnar plus equiaxed, and equiaxed

(isotropic grain morphology). A higher solidification rate typically causes transition from columnar to mixed/equiaxed grain morphology[33] and increasing the cooling rate usually leads to finer microstructure.[20,37] For instance, the macrostructure of laser-deposited Ti-6Al-4V consists of columnar prior-β grains elongated in the solidification (build) direction as presented in Fig. 6a. The microstructure includes very fine Widmanstätten platelet α (basket weave or colony structures of α phase lamellae in a β matrix), as shown in Fig. 6b. This has been explained by the rapid cooling rate after the solidification stage.[32,38] To eventually fabricate Ti-6Al-4V parts with enhanced mechanical properties, it is essential to effectively optimize and control the effect of process parameters on microstructure.

Distinct microstructure regions with different microhardnesses have been reported for Ti-6Al-4V/ DLD.[39] This variation can be attributed to the high temperature gradients, different cooling rates, and repeated thermal cycling experienced during DLD and the layer-to-layer massification process. Higher microhardness has been measured at the bottom and top of DLD parts, which may be due to the (I) higher cooling rate of the melt pool and velocity of solidification at the top and bottom regions, which results in a finer microstructure, and (II) the cyclic reheating from the subsequent deposited layers in middle regions. The cyclic reheating and lower cooling rates in the middle region may result in tempering and aging, and therefore, a coarser microstructure.[36] As a result of different thermal histories, the sizes of the α and β laths of the laser-deposited Ti-6Al-4V samples have been reported to vary with location.[36,39] Although the Widmanstätten microstructure exists at the top and bottom of Ti-6Al-4V/DLD parts, the microstructural morphology of each region is different; the top region consists mostly of colonies of parallel, very fine lamellae, and larger laths, and the bottom region has a much thicker lamellae structure.[39]

Thermal transients and gradients, as well as repeated rapid heating and cooling during the building process, are known to cause residual stresses in the DLD fabricated Ti-6Al-4V parts.[40,41] Material properties (i.e., the thermal conductivity, CTE, elastic modulus and yield stress), phase transformation, part geometry, process parameters and scanning pattern influence the magnitude and formation pattern of residual stress within DLD-fabricated titanium parts.[42] Residual stresses are important to acknowledge because they may reduce the fatigue resistance of DLD parts and also cause warping, resulting in dimensional inaccuracies.[42]

The resultant residual stresses in DLD-produced materials depend on the tensile properties (i.e., monotonic stress–strain behavior) and the temperature-induced strain mismatch in the part during the post-manufacturing cooling stage. Materials with higher yield stresses usually promote the existence of residual stresses with higher magnitude. The material's yield stress–temperature curve is yet another important, determining factor. Materials with high yield strength at elevated temperatures, such as superalloys (e.g., Inconel 718), produce greater residual stresses due to the lack of plastic flow for facilitating thermally induced volume changes.[40] Ti-6Al-4V/DLD parts are also susceptible to a high level of residual stresses due to their high yield strength at elevated temperatures.

The residual stresses of Ti-6Al-4V have been reported to be aligned with the laser scanning direction; compressive residual stresses are located at the center and tensile residual stresses at the edges of the parts.[43] The lowest residual stresses are typically observed to be at the starting point of laser scanning and the largest residual stresses are at the end of the laser scanning path.[43] Compressive residual stresses are larger near the substrate and gradually change to tensile residual stresses at the top of the sample.[43] Tensile residual stresses are extremely detrimental on fatigue resistance of
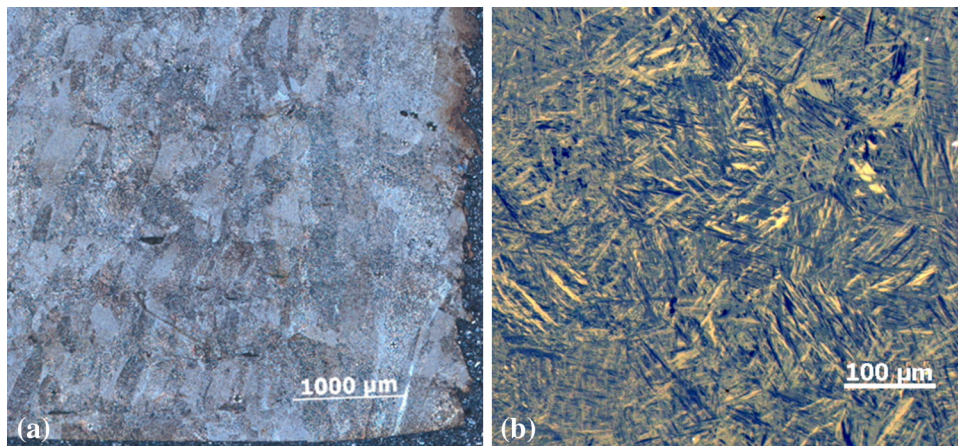

Fig. 6. (a) Macrostructure with fine columnar grains and (b) microstructure containing very fine Widmanstätten structure for LENS-produced Ti-6Al-4V.

Ti-6Al-4V as they typically allow fatigue cracks to grow at the surface and tend to open the fatigue crack, reduce friction, and accelerate fatigue damage. To reduce residual stresses and distortion, the DLD process should be optimized and controlled properly (e.g., controlling laser power and beam traverse speed). In addition, preheating the substrate and previously deposited layers (to establish a more uniform temperature distribution), maintaining optimal melt pool shape, and using a proper scanning pattern are other methods for reducing residual stresses in DLD-produced parts.[40,42,44] Manipulating the process parameters to maintain constant melt pool size and temperature throughout the part, especially at the corners (layer start/finish), leads to reduction in residual stresses.[40,42] Choosing the proper scanning patterns reduces thermal stresses and the resulting thermal distortions.

EFFECTS OF PROCESS PARAMETERS

Process parameters such as laser power P, laser beam radius r, and relative traverse speed/velocity v control the incident specific energy ($E = P/(2rv)$ in units J/mm^3). Specifically, these parameters strongly dictate the melt pool geometry (i.e., size, shape, and depth), which subsequently affects the thermal gradients and cooling rates. Higher laser powers or lower traverse speeds result in higher specific energies and, consequently, a higher cooling rate as well as finer microstructure, and vice versa.[12,33,36] Lower incident energy results in finer equiaxed morphologies, whereas increasing incident energy generally results in a coarser microstructure and columnar grains.[36] For a thin wall of Ti-6Al-4V/DLD, transition from columnar to mixed equiaxed-columnar microstructure has been observed at the surface of the deposit[33] because the cooling rate, and thus the solidification rate, increase gradually along this direction. Moreover, increasing powder feed rate results in a coarser microstructure (i.e., an increase in the width and length of both α and β laths) for Ti-6Al-4V/DLD. At higher laser powers, the feed rate has less effect. A slight decrease in the size of α and β laths is also observed with an increase in the traverse velocity.

The majority of incident energy is dissipated by conduction through the deposited structure, thus impacting the microstructural evolution within the DLD part.[32] At the bottom of the part, heat quickly conducts away through the substrate, whereas, convection and radiation become more dominant at the top.[36] Columnar grains have been observed to form across the deposited layers, indicating the epitaxial growth of dendrites from the substrate or previously deposited layers.[36] As a result of higher cooling rates, a finer and more equiaxed microstructure with primary dendrites usually exists at the bottom and the top of the deposited part. For example, the microstructure of Ti-6Al-4V, as a result of rapid cooling rate, includes very fine

Widmanstätten platelet α as presented in Fig. 6b. Similar structures have also been observed for each deposited layer, composed of two regions with distinct dendrite features. Due to higher cooling rates and the solidification speed of the melt pool, the bottom of each layer is mostly columnar with no associated secondary dendrites. The top part of each layer consists of a fine equiaxed structure with secondary dendrite arms due to a typically lower cooling rate and, consequently, a lower solidification speed of melt pool. As a result of remelting and heating effects of the previously deposited layers, the grain size at the bottom of the solidified melt pool is coarser than the one at the top.[45,46]

Microstructure with alternating sublayers may occur as a result of partial remelting between layers.[47] When one layer is being deposited, remelting can occur in the top portion of the previous layer, resulting in a coarsening of the particles; the bottom portion of the previous layer is only reheated, which has less effect on grain growth. Reheating of previously solidified material in the middle of the part results in slower cooling rates that favor the formation of secondary dendrites.[36] These thermal cycles can also activate a variety of metallurgical phenomena that progressively modify the microstructural properties such as grain size.[22] The difference in the thermal history at each point of the deposited part causes heterogeneous behavior in the microstructure, which affects other mechanical properties such as tensile and fatigue resistance.[48] To resolve the consequential inhomogeneity in the microstructure caused by remelting and thermal cycling, laser parameters should be adjusted during the deposition of each layer so that the temperature of the layer below the new layer remains below the eutectic temperature.

The amount of powder forming a layer is mainly determined by the amount of powder injected into the melt pool, characterized by the deposited mass flow rate (powder feed rate) and the material stream concentration distribution. The resulting distribution of powder density in the melt pool is an essential factor to layer thickness and thus microstructure.[49] Thus, it is very important to understand the effects of process parameters on the amount of the powder injected into the melt pool and its distribution.

The powder feed rate has a direct impact on the distribution of powder density and thus layer thickness. In general, there exists a linear increase in the layer thickness as the powder feed rate increases,[14] which in turn results in a coarser microstructure. However, the effect of the powder feed rate interacts with other parameters, such as laser power, resulting in laser attenuation effects. Higher laser power coupled with a lower powder feed rate results in equiaxed microstructure with high porosity; on the other hand, smaller laser powers with large powder feed rates correspond to columnar microstructure.

Even for a fixed powder feed rate, the amount of powder injected into the melt pool varies for different laser scanning directions because of the gap between the laser spot and powder stream. The shape of the melt pool is generally not symmetric; the leading part of the melt pool is smaller than its tail due to the heat flux variation.[50] Depending on scanning directions, the powder injection point may be ahead of or behind the laser spot. Because only the portion of powder stream that is overlapped with laser beam is melted, different scanning directions may result in different layer thicknesses. This issue is further compounded by the fact that the relative position of the laser beam and powder injection point change as the surface of the substrate is lifted due to deposition.

The flow rate of shielding gas also affects the amount of powder injected into the melt pool. Experimental studies demonstrate that as the gas flow rate increases, the powder density and layer thickness first increase and then eventually decrease. This is partially because increasing the shielding gas flow rate improves the amount of powder injected into melt pool. Faster particle streams, however, eventually lead to mass reflection at the melt pool, thus decreasing powder efficiency.

The orientation of the part during DLD may affect its post-build mechanical properties. For instance, it has been reported that deposition in the direction along (i.e., horizontal) the length of samples typically exhibits higher tensile strength than having their layers deposited perpendicularly (i.e., vertically), as presented in Fig. 3. This anisotropic behavior can be attributed to the weak interfacial layers being parallel to crack propagation, in the vertical direction, providing an easy path for shear bands.[23,32] Different cooling rates for these two deposition orientations may also influence the microstructure and mechanical properties. For deposited samples in the horizontal direction, the laser passing time between each successive layer can be longer than parts with deposition in the vertical direction. Hence, vertically built parts can have higher cooling rates, and consequently, finer microstructures.[51]

Conventional DLD processes use a computer-drafted model that represents the part via multiple, parallel layers. Whereas this layer-to-layer construction method results in good part quality for parts with simple shapes, it leads to the so-called "staircase effect" when fabricating parts with relatively complex geometry. Because of the finite thickness of a deposition layer, surfaces whose normal vectors do not make an angle of either 0° or 90° with the build direction can only be deposited approximately. The magnitude of the staircase effect is dependent on the layer thickness and the angle made by the surface normal with the build direction. This results in poor surface quality and requires post-processing to form the desired shape, which increases the overall process time. Some have

investigated the effect of tool path by attempting to minimize staircase effects, e.g., controlling layer thickness[52] and volumetric difference.[53] However, these approaches are based on fixed deposition direction and, thus, do not eliminate the staircase effect. Multi-axis processing is another alternative to mitigate the staircase effect. Instead of adopting the traditional parallel slicing approach, multi-axis processing rotates the slicing direction for 90° when an overhang structure occurs.[54,55] However, collision with previously deposited layers may still occur when rotating the part by 90°. To address this challenge, a non-parallel layer slicing strategy that allows the deposition to follow the geometry of a part more precisely by Ruan et al.[56]

It is clear that due to the complex, coupled thermophysical dynamics associated with the DLD process, process parameters need to be adjusted in real time to ensure that desired mechanical/microstructural properties can be obtained. This is in direct contrast to the traditional "set-it-and-forget-it," open-loop DLD process that consists of time-invariant process parameters. Currently, the majority of existing DLD control processes focus on maintaining constant melt pool morphology/temperature and deposited layer height.

The effect of DLD process parameters on part temperature and mechanical properties, such as the laser beam traverse speed, laser power, specific energy, powder feed rate and substrate thickness, has been experimentally and numerically investigated extensively in the past several years. Many general conclusions regarding the uncontrolled, time-invariant DLD process parameters on the overall part/structure are now well accepted, for example:

1. The melt pool will elongate and become thinner with faster traverse speeds and higher laser powers.[15,57]
2. Later layers will tend to be thinner and blossom out, i.e., "mushrooming."[58,59]
3. Substrate thickness will impact the part heat transfer and microstructure near the substrate-part junction.[58,60]
4. Deposition/layer thickness will increase with delivered specific energy.[14]
5. Higher powder feed rates will decrease the depth of the melt pool[61] while increasing layer height.[50]

While there are many other conclusions one may draw from DLD process parameters, based on the previous five conclusions alone, real-time control methods are needed to ensure desirable part during the build.

SUMMARY

This article has focused on the microstructure, post-manufacturing characteristics, and tensile/fatigue properties of parts fabricated via DLD, which is a laser-based AM process. The microstructure and

mechanical properties of parts fabricated with Ti-6Al-4V using DLD (e.g., Ti-6Al-4V/DLD) were specifically highlighted and related to the various effects of the DLD and post-DLD (e.g., heat treatment) process parameters. During DLD, the combination of the various process parameters—such as laser power, traverse speed, powder feed rate, etc.—and process uncertainties, results in the deposited parts experiencing a complex thermal history. Nonuniform/transient thermal gradients experienced during primary-dendritic solidification of Ti-6Al-4V cause the formation of undesirable residual stresses and distortions within DLD parts. Material tensile and thermal properties, phase transformation, part geometry, process parameters, and scanning pattern have been reported to influence the magnitude and pattern of the residual stress in Ti-6Al-4V/DLD.

The melt pool specific to Ti-6Al-4V can consist of surface-tension and free-convection flows along its free-surface periphery and is more prone to oxidization. The microstructure (e.g., sizes of the α and β laths), microhardness, and residual stresses have been reported to vary along (uncontrolled) Ti-6Al-4V/DLD parts and this heterogeneity is shown to depend on layer-to-substrate distance and thermal cycling. High cooling rates for DLD can be achieved as to generate fine microstructures; however, laser idling (or other forms of DLD control) may need to be imposed as to guarantee consistent cooling rates for each layer.

In order to achieve the desired microstructure needed for Ti-6Al-4V/DLD parts with enhanced mechanical properties, the DLD process parameters should be properly optimized and controlled. This may be achieved by controlling laser power and traverse speed, preheating the substrate and previously deposited layers to achieve a more uniform temperature distribution, and using a proper scanning pattern. However, more recent studies show that the melt pool area may not be a sufficient indicator to achieve desired part quality.[62] Other process variables, such as layer height and bulk part temperature, should be monitored and controlled simultaneously.

Tensile properties (including the yield and tensile strengths) of Ti-6Al-4V/DLD parts are typically similar, or even superior, to those of their wrought counterparts as a result of the high cooling rates experienced during the DLD process. However, less elongation to failure and ductility has been reported.

Inconsistent results have been reported in the literature for fatigue behavior of Ti-6Al-4V/DLD specimens. Such inconsistencies may be attributed to different microstructures and porosity levels resulting from different manufacturing/post-manufacturing process parameters. Manufacturing process parameters, such as laser power, laser beam traverse speed, powder feed rate, layer thickness, etc. greatly influence the thermal history, microstructure

(morphology and volume fraction of α and β constituents), residual stresses, bonding between layers, pore size and shape, affecting the fatigue resistance of the Ti-6Al-4V/DLD parts. Selecting the process parameters for achieving the desired/targeted fatigue behavior requires further investigation.

Anisotropic mechanical behavior has been reported in tensile and fatigue properties of Ti-6Al-4V/DLD parts as the vertically built parts typically have lower tensile properties (i.e., ultimate and yield strengths as well as elongation to failure) and fatigue resistance as compared to the horizontally built parts. This can be explained by the vertically and horizontally built specimens having multi-directional and inhomogeneous cooling rates, which results in different microstructural features, residual stresses, and fatigue behaviors. In addition, extensive porosity has been reported in parts fabricated in the vertical direction relative to those built in the horizontal direction. Such anisotropic behavior in tensile and fatigue properties may be significantly reduced by post-fabrication machining as well as proper heat treatments, specifically HIP. The HIP process densifies the material, reduces the porosity, and results in a higher ductility, elongation to rupture, and fatigue life.

REFERENCES

1. W.U.H. Syed, A.J. Pinkerton, and L. Li, *Appl. Surf. Sci.* 252, 4803 (2006).
2. F. Wang, J. Mei, and X. Wu, *Mater. Des.* 28, 2040 (2007).
3. M.L. Griffith, M.E. Schlienger, L.D. Harwell, M.S. Oliver, M.D. Baldwin, M.T. Ensz, J.E. Smugeresky, M. Essien, J. Brooks, C.V. Robino, W.H. Hofmeister, M.J. Wert, and D.V. Nelson, *Paper presented at the Proceedings of the 9th Solid Freeform Fabrication Symposium* (Austin, TX, 1998), pp. 89–96.
4. L. Tang and R.G. Landers, *ASME J. Manuf. Sci. Eng.* 132, 011010 (2010).
5. M. Griffith, M. Schlienger, L. Harwell, M. Oliver, M. Baldwin, M. Ensz, M. Essien, J. Brooks, C. Robino, J. Smugeresky, W. Hofmeister, M. Wert, and D. Nelson, *Mater. Des.* 20, 107 (1999).
6. T.A. Davis (M.Eng. thesis, University of Louisville, 2004).
7. G. Pi, A. Zhang, G. Zhu, D. Li, and B. Lu, *Int. J. Adv. Manuf. Technol.* 57, 841 (2011).
8. L. Han, K.M. Phatak, and F.W. Liou, *Metall. Mater. Trans. B* 35, 1139 (2004).
9. N. Shamsaei, M. Gladskyi, K. Panasovskyi, S. Shukaev, and A. Fatemi, *Int. J. Fatigue* 32, 1862 (2010).
10. F.P. Jeantette, D.M. Keicher, J.A. Romero, and L.P. Schanwald, U.S. patent US006046426A (2000).
11. X. He and J. Mazumder, *J. Appl. Phys.* 101, 053113 (2007).
12. B. Zheng, Y. Zhou, J.E. Smugeresky, J.M. Schoenung, and E.J. Lavernia, *Metall. Mater. Trans. A* 39, 2228 (2008).
13. S. Wen and Y.C. Shin, *J. Appl. Phys.* 108, 044908 (2010).
14. J. Mazumder, A. Schifferer, and J. Choi, *Mater. Res. Innov.* 3, 118 (1998).
15. L. Wang, S.D. Felicelli, and J.E. Craig, *J. Manuf. Sci. Eng.* 131, 041019 (2009).
16. J.E. Craig, T. Wakeman, R. Grylls, and J. Bullen, *Paper presented at the TMS 2011 Annual Meeting and Exhibition* (San Diego, CA, 2011).
17. J.J. Hammell, C.J. Ludvigson, M.A. Langerman, and J.W. Sears, *Paper presented at the ASME 2011 International Mechanical Engineering Congress and Exposition* (Denver, CO, 2011), pp. 41–48.

18. J. Koch and J. Mazumder, U.S. patent US6122564A (2000).
19. M.L. Griffith, W.H. Hofmeister, G.A. Knorovsky, D.O. MacCallum, M.E. Schlienger, and J.E. Smugeresky, US patent US6459951B1 (2002).
20. W. Hofmeister, M. Griffith, M. Ensz, and J. Smugeresky, *JOM* 53, 30 (2001).
21. P. Peyre, P. Aubry, R. Fabbro, R. Neveu, and A. Longuet, *J. Phys. D Appl. Phys.* 41, 025403 (2008).
22. L. Costa and R. Vilar, *Rapid Prototyp. J.* 15, 264 (2009).
23. P.A. Kobryn and S.L. Semiatin, *Paper presented at the Proceedings of the 12th Solid Freeform Fabrication* (Austin, TX, 2001), p. 179.
24. R. Grylls, Optomec Intern. Report, Addit. Manuf. Syst. Nano MACRO 2 (2005).
25. W. Chen, C. Boehlert, J. Howe, and E. Payzant, *Metall. Mater. Trans. A* 42, 3046 (2011).
26. H.K. Rafi, T.L. Starr, and B.E. Stucker, *Int. J. Adv. Manuf. Technol.* 69, 1299 (2013).
27. Y. Wang, S. Zhang, X. Tian, and H. Wang, *Int. J. Miner. Metall. Mater.* 20, 665 (2013).
28. F. Wang, *Int. J. Adv. Manuf. Technol.* 58, 545 (2011).
29. C. Lin, C. Ju, and J.C. Lin, *Biomaterials* 26, 2899 (2005).
30. G. Dinda, L. Song, and J. Mazumder, *Metall. Mater. Trans. A* 39, 2914 (2008).
31. K. Dragolich, N. DiMatteo, and S. Henry, *Fatigue Data Book: Light Structural Alloys* (Materials Park, OH: ASM International, 1994).
32. J. Alcisto, A. Enriquez, H. Garcia, S. Hinkson, T. Steelman, E. Silverman, P. Valdovino, H. Gigerenzer, J. Foyos, J. Ogren, J. Dorey, K. Karg, T. McDonald, and O.S. Es-Said, *J. Mater. Eng. Perform.* 20, 203 (2010).
33. S. Bontha, N.W. Klingbeil, P.A. Kobryn, and H.L. Fraser, *J. Mater. Process. Technol.* 178, 135 (2006).
34. S. Bontha, N.W. Klingbeil, P.A. Kobryn, and H.L. Fraser, *Mater. Sci. Eng. A* 513–514, 311 (2009).
35. R. Vilar, *J. Laser Appl.* 11, 64 (2001).
36. C. Selcuk, *Powder Metall.* 54, 94 (2011).
37. W. Hofmeister, M. Wert, and J. Smugeresky, *JOM* 51, 1 (1999).
38. M. Hedges and N. Calder, *Paper presented at the Cost Effective Manufacturing via Net-Shape Processing Meeting Proceedings RTO-MP-AVT-139 13* (2006).
39. B. Baufeld, O. Van Der Biest, R. Gault, and K. Ridgway, *IOP Conf. Ser. Mater. Sci. Eng.* 26, 012001 (2011).
40. P. Rangaswamy, M.L. Griffith, M.B. Prime, T.M. Holden, R.B. Rogge, J.M. Edwards, and R.J. Sebring, *Mater. Sci. Eng. A* 399, 72 (2005).
41. F. Liu, X. Lin, G. Yang, M. Song, J. Chen, and W. Huang, *Opt. Laser Technol.* 43, 208 (2011).
42. J. Beuth and N. Klingbeil, *JOM* 53, 36 (2001).
43. Z. Shuangyin, L. Xin, C. Jing, and H. Weidong, *Rare Met. Mater. Eng.* 38, 774 (2009).
44. K. Dai and L. Shaw, *Rapid Prototype J.* 8, 270 (2002).
45. G.P. Dinda, A.K. Dasgupta, and J. Mazumder, *Mater. Sci. Eng. A* 509, 98 (2009).
46. B. Zheng, Y. Zhou, J.E. Smugeresky, J.M. Schoenung, and E.J. Lavernia, *Metall. Mater. Trans. A* 39, 2237 (2008).
47. Y. Xiong, W.H. Hofmeister, Z. Cheng, J.E. Smugeresky, E.J. Lavernia, and J.M. Schoenung, *Acta Mater.* 57, 5419 (2009).
48. D. Keicher and J. Smugeresky, *JOM* 49, 51 (1997).
49. Y. Li, H. Yang, X. Lin, W. Huang, J. Li, and Y. Zhou, *Mater. Sci. Eng. A* 360, 18 (2003).
50. A.J. Pinkerton and L. Li, *J. Phys. D Appl. Phys.* 37, 1885 (2004).
51. P.L. Blackwell, *J. Mater. Process Technol.* 170, 240 (2005).
52. A. Dolenc and I. Mäkelä, *Comput. Des.* 26, 119 (1994).
53. Y. Yang, J.Y.H. Fuh, H.T. Loh, and Y.S. Wong, *J. Manuf. Sci. Eng.* 125, 586 (2003).
54. P. Singh and D. Dutta, *J. Comput. Inf. Sci. Eng.* 1, 129 (2001).
55. Y. Yang, J.Y.H. Fuh, H.T. Loh, and Y.S. Wong, *IEEE Trans. Autom. Sci. Eng.* 2, 276 (2005).
56. J. Ruan, L. Tang, F.W. Liou, and R.G. Landers, *J. Manuf. Sci. Eng.* 132, 064502 (2010).
57. L. Wang, S. Felicelli, Y. Gooroochurn, P.T. Wang, and M.F. Horstemeyer, *Mater. Sci. Eng. A* 474, 148 (2008).
58. L. Costa, R. Vilar, T. Reti, and A.M. Deus, *Acta Mater.* 53, 3987 (2005).
59. M. Alimardani, E. Toyserkani, and J.P. Huissoon, *J. Laser Appl.* 19, 14 (2007).
60. M.L. Griffith, D.M. Keicher, C.L. Atwood, J.A. Romero, J.E. Smugeresky, L.D. Harwell, and D.L. Greene, *Paper Presented at the Proceedings of the 7th Solid Freeform Fabrication Symposium* (Austin, TX, 1996), pp. 125–132.
61. F. Vásquez, J.A. Ramos-Grez, and M. Walczak, *Int. J. Adv. Manuf. Technol.* 59, 1037 (2012).
62. A. Raghavan, H.L. Wei, T.A. Palmer, and T. DebRoy, *J. Laser Appl.* 25, 052006 (2013).
63. M. Donachie, *Titanium: A Technical Guide* (Materials Park, OH: ASM Int., 2000).